



## ORIGINAL ARTICLE

# Phenotypic plasticity at the edge: Contrasting population-level responses at the overlap of the leading and rear edges of the geographical distribution of two *Scurria* limpets

Bernardo R. Broitman<sup>1,2</sup> | Moisés A. Aguilera<sup>2</sup> | Nelson A. Lagos<sup>3</sup> | Marco A. Lardies<sup>4</sup>

<sup>1</sup>Centro de Estudios Avanzados en Zonas Áridas, Coquimbo, Chile

<sup>2</sup>Departamento de Biología Marina, Facultad de Ciencias del Mar, Universidad Católica del Norte, Coquimbo, Chile

<sup>3</sup>Centro de Investigación e Innovación para el Cambio Climático (CiiCC), Facultad de Ciencias, Universidad Santo Tomás, Santiago, Chile

<sup>4</sup>Facultad de Artes Liberales, Universidad Adolfo Ibáñez, Santiago, Chile

**Correspondence**

Bernardo R. Broitman, Centro de Estudios Avanzados en Zonas Áridas, Coquimbo, Chile.  
Email: bernardo.broitman@ceaza.cl

**Funding information**

Fondo Nacional de Desarrollo Científico y Tecnológico, Grant/Award Number: 1140092, 1140938, 1160223, ICM Nucleus MUSELS, PAI-CONICYT 79150002

Editor: Alistair Crame

**Abstract**

**Aim:** To examine the role of ocean temperature and chemistry as drivers of inter-population differences in multiple phenotypic traits between rear and leading edge populations of two species of limpet.

**Location:** The coast of north-central Chile, western South America.

**Taxon:** Mollusca, Gastropoda (Lottidae).

**Methods:** We used field and laboratory experiments to study the ecology and physiology of individuals from populations located at the overlap of the rear and leading edges of their respective geographical distributions. At the same time, we characterized local environmental regimes, measuring seawater physical and chemical properties.

**Results:** Towards the edge of their range, individuals from the leading edge species gradually reduced their shell length, metabolic rate and thermal response capacity, and increased carbonate content in their shells. Individuals of the rear edge species showed dissimilar responses between sites. Contrasting behavioural responses to experimental heating reconciled observations of an unintuitive higher maximal critical temperature and a smaller thermal safety margin for individuals of the rear edge populations. Physical–chemical characterization of seawater properties at the site located on the core of the upwelling centre showed extreme environmental conditions, with low oxygen concentration, high pCO<sub>2</sub> and the episodic presence of corrosive seawater. These challenging environmental conditions were reflected in reduced growth for both species.

**Main conclusions:** We found different spatial patterns of phenotypic plasticity in two sister species around the leading and trailing edges of their distributions. Our results provide evidence that environmental conditions around large upwelling centres can maintain biogeographical breaks through metabolic constraints on the performance of calcifying organisms. Thus, local changes in seawater chemistry associated with coastal upwelling circulation emerge as a previously overlooked driver of marine range edges.

**KEYWORDS**

biogeographical break, calcification, limpet, *Scurria*, SE Pacific, thermal physiology, upwelling

## 1 | INTRODUCTION

Geographical range boundaries are the result of an interplay between environmental and eco-evolutionary processes (Brown, Stevens, & Kaufman, 1996; Peterson et al., 2011). Biogeographical provinces in the coastal ocean today are largely a result of historical processes that established large-scale patterns in species composition through diversification within and between regions (Bowen et al., 2016). Insights into the organismal and ecological mechanisms maintaining coastal geographical range boundaries have only come forward recently (Lima, Queiroz, Ribeiro, Hawkins, & Santos, 2006; Seabra, Wetthey, Santos, Gomes, & Lima, 2016; Wetthey, 1983), with much of the interest fuelled by the climate-driven, poleward range expansion of warm-temperate marine taxa (Somero, 2010). On the other hand, range contractions are taking place at the equatorward, or rear edge of species' geographical distributions, where locally adapted populations undergo extinction as the environmental regime changes beyond their physiological limits (Hampe & Petit, 2005; Hewitt, 2000). Populations at the rear edge of the range will display between-site differences in adaptive responses as population-level performance has been tuned by natural selection to track local conditions, while populations at the leading edge will show a steady decrease in performance towards the range edge (Hampe & Petit, 2005; Kawecki & Ebert, 2004). Thus, comparing organismal and ecological processes between leading and rear range edges can provide important insights into our basic understanding of the drivers of geographical range dynamics. Such comparisons remain exceedingly rare, particularly in marine systems (Nicastro et al., 2013; Zardi et al., 2015).

Coastal upwelling along the mid-latitude eastern margins of oceans is a circulation process where the wind-driven, equatorward alongshore flow of surface water is advected offshore through the Coriolis Effect and replaced by subsuperficial waters (Hill et al., 1998). The clustering of biogeographical breaks around major eastern boundary upwelling centres, such as Point Conception in western North America (Blanchette et al., 2008), is broadly attributed to the offshore advection of planktonic larvae entrained in the divergent flow field around these prominent topographic or bathymetric features (Gaylord & Gaines, 2000). The high primary productivity characteristic of upwelling regions is maintained by the emergence of nutrient-rich waters from the subsurface (Hill et al., 1998), which are also cold, supersaturated in CO<sub>2</sub>, with low O<sub>2</sub> concentration and low pH (Feely, Sabine, Hernandez-Ayon, Janson, & Hales, 2008; Kapsenberg & Hofmann, 2016). The presence of cool waters and the onshore cloudiness characteristic of coastal upwelling ecosystems maintain mild atmospheric conditions on the shoreline (Falvey & Garreaud, 2009; Hill et al., 1998). However, the demanding physico-chemical properties of coastal ocean waters around upwelling centres suggest that local environmental conditions can play an important role as a driver of geographical range edges for calcifying organisms (Ramajo et al., 2016). Despite the possibility that local environmental conditions define the range edge of coastal marine

populations, this mechanism remains largely untested, with most of the theory and evidence pointed towards dispersal-based mechanisms (Gaylord & Gaines, 2000; Lima et al., 2006).

Rocky intertidal invertebrates provide a model system to study the effects of local environmental conditions because of their reduced mobility and temporary exposure to marine and terrestrial or semi-terrestrial conditions (Helmuth, Mieszowska, Moore, & Hawkins, 2006). Adaptation to local conditions is mirrored by the pattern of variability in the performance of a given phenotypic trait between extremes in the environment, a reaction norm, which can be evaluated for a suite of traits such as heat and water stress (Williams et al., 2011), behaviour (Woods, Dillon, & Pincebourde, 2015), or the capacity of calcifying organisms to deposit and maintain calcareous exoskeletons (Duarte et al., 2014; Ramajo et al., 2016). Species of the gastropod genus *Scurria* (Lottiidae) are only found along the rocky shores of the south-eastern Pacific upwelling system and provide an ideal model system to examine the effects of environmental conditions. This diverse group of limpets share an evolutionary history defined by the exposure to coastal upwelling waters, together with similar ecological and life history characteristics (Espoz, Lindberg, Castilla, & Simison, 2004). Here, we examine the plastic phenotypic responses of two *Scurria* species around a biogeographical break associated with a large upwelling centre where the rear and leading edges of two sister species overlap (Aguilera, Valdivia, & Broitman, 2013). Using physical-chemical monitoring and laboratory and field experiments, we examine the interpopulation variability in behavioural, morphological, physiological, and metabolic responses of both species and test the general hypothesis of differences in the pattern of population-level phenotypic responses between rear and leading edge populations around their shared biogeographical break. Finally, we discuss the implications of our results for the stability of biogeographical boundaries in coastal upwelling ecosystems worldwide.

## 2 | MATERIALS AND METHODS

### 2.1 | Study populations and model species

Along the north-central coast of Chile, a major oceanographic and biogeographical break is associated with a large headland, Punta Lengua de Vaca, located ~30° S (PLV, Figure 1a). We selected four study sites, Talcaruca (30°29' S, 71°41' W), which is located on the core of the PLV upwelling centre and biogeographical break, and three other sites located outside the influence of PLV as controls: Los Molles (32°33' S, 71°32' W) and El Tabo (33°27' S, 71°88' W) to the south of PLV, and Huasco (28°24' S, 71°13' W), to the north (Figure 1a). To test our hypothesis, we selected the limpet *Scurria viridula* (Lamarck 1819), with a reported poleward range endpoint ~150 km south of PLV (Espoz et al., 2004; Rivadeneira & Fernández, 2005), which has been recently reported to occur further south (Aguilera et al., 2013), and *Scurria zebrina* (Lesson 1830), with an equatorward range endpoint ~50 km north of PLV, well within the

influence of the strong upwelling off PLV. The biology of these free-living molluscs is only partially known and they are commonly found in the middle intertidal zone of rocky shores, and although their geographical ranges overlap for only ~200 km, *S. viridula* and *S. zebrina* are sister species (Espoz et al., 2004).

## 2.2 | Animal collection

Animals were collected randomly by hand at low tide during 2014 and 2015 from the rocky intertidal area at all study sites. To remove possible confounding effects of sex, only small juvenile limpets (males) were used in experiments and for physiological measurements. Individuals were chilled and transported to the laboratory, where they were acclimated at constant temperature ( $14 \pm 1^\circ\text{C}$ ) in artificial seawater (ASW; 33 ppm; Instant Ocean© sea salt dissolved in distilled water) under a simulated semidiurnal tidal cycle, kept for one month exposed to a 12 h:12 h light:dark cycle and fed *Ulva* spp. three times a week.

## 2.3 | Variability of in situ seawater temperature, air temperature, and carbonate system parameters

To characterize ocean temperature patterns at each site, we used data from an ongoing long-term monitoring program (Aravena,

Broitman, & Stenseth, 2014). Briefly, we installed submersible temperature data loggers (HOBO®, Onset Computer Corp., MA, USA) housed inside PVC pipes embedded in concrete blocks attached to a chain bolted to the shoreline and deployed ~1 m below the surface. The loggers record ocean temperature data every 20 min, which is downloaded on a monthly or seasonal schedule; data details and availability are presented elsewhere (Tapia, Largier, Castillo, Wieters, & Navarrete, 2014). Data for local temperature climatology (Figure 1b) are long-term daily averages, and all sites have between 6 and 13 years of high-frequency data. As our southernmost *S. viridula* population was detected at El Tabo, a location not included in the long-term temperature monitoring program, we used the long-term record from the Estación Costera de Investigaciones Marinas (ECIM), which is located ~10 km south of El Tabo (green square in Figure 1a). To obtain a synoptic view of temperature variability across the PLV biogeographical break, we used mapped, 8-day, Level-3 night-time sea surface temperature (SST) records from the MODerate Resolution Imaging Spectroradiometer (MODIS) at 4 km resolution for the 2003–2016 period to examine the spatial variance in the SST field across the region and among-site temperature climatology. MODIS records were downloaded from the NASA Ocean Colour repository and all analyses carried out in MatLab R2013a. In addition, we examined air temperature along the coast of Chile using

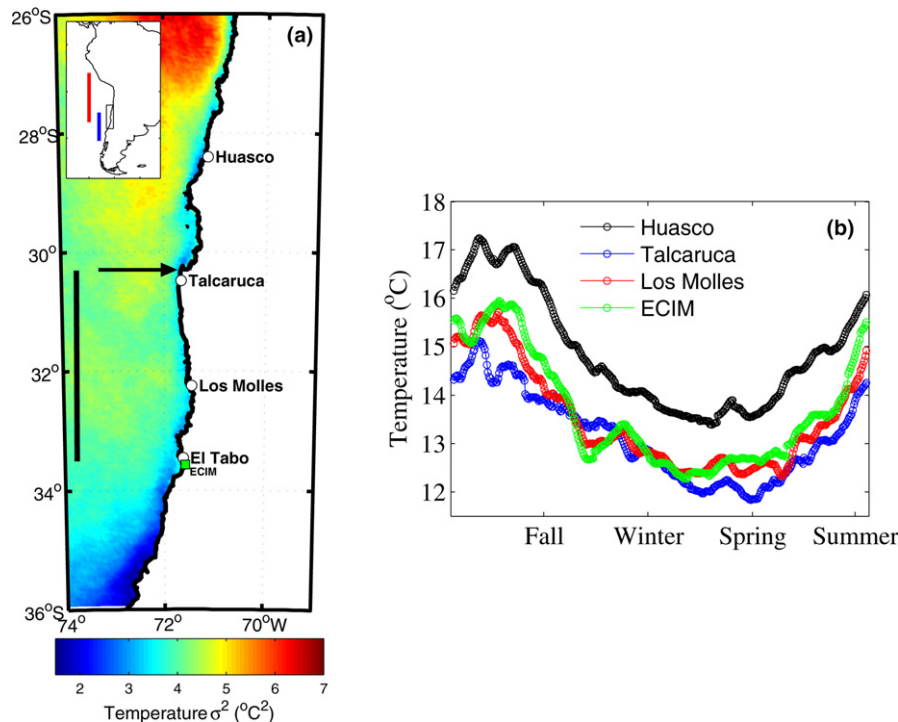


**FIGURE 1** (a) Map of the study region along north-central Chile, where colours on the ocean satellite image illustrate the spatial pattern of SST variance ( $^{\circ}\text{C}^2$ ), the location of the four study sites (open circles) and a nearby marine station (ECIM, green square) from where we obtained the temperature record used for our southernmost location, El Tabo. The location of the Punta Lengua de Vaca headland (PLV), which is immediately above the Talcaruca site, is indicated by a black arrow. The overlap of the leading edge of *Scurria viridula* and the trailing edge of *Scurria zebrina* is depicted by a vertical black line on the left of the figure. The inset on the upper left corner is a map of western South America showing the latitudinal extent of geographical ranges of *S. viridula* (red, from 12 to 32° S, recently expanded to 33.5° S, Aguilera et al., 2013) and *S. zebrina* (blue, from 30.5 to 42° S). The small rectangle in the inset corresponds to the study region shown in the main map. (b) Climatology of in situ records of ocean temperature showing the long-term mean daily values at the four study sites

published long-term records from coastal meteorological stations, usually lighthouses or harbours (Di Castri & Hajek, 1976; Lardies, Muñoz, Paschke, & Bozinovic, 2011). For pH measurements (total scale), two water samples were collected and analysed within 60 min of collection, using a Metrohm 826 pHMobile Meter<sup>®</sup> connected to a combined electrode (double juncture), calibrated using TRIS buffers (pH = 8.089) at 25°C using a thermo-regulable water bath. For total alkalinity ( $A_T$ ) analyses, discrete water samples were collected using borosilicate glass bottles (Corning 500-mL), poisoned using mercuric chloride (0.2 cm<sup>3</sup> of a 50% saturated solution) and sealed with Apiezon<sup>®</sup> L grease for transportation to the laboratory. Samples were stored for no more than 3 months in cool, dark conditions until analysis. Three to five seawater subsamples of each bottle were used to estimate measurement of  $A_T$  using automated potentiometric titration (Haraldsson, Anderson, Hassellöv, Hulth, & Olsson, 1997). Partial pressure of CO<sub>2</sub> ( $pCO_2$ ) and saturation states ( $\Omega$ ) for calcite and aragonite were estimated from the averaged values of pH<sub>T</sub>,  $A_T$  and SST using the co2sys software (Pierrot, Lewis, & Wallace, 2006).

## 2.4 | Thermal responses: behavioural field experiments

In order to explore the in situ thermal responses of the *Scurria* limpets, we conducted a short-term field experiment at Limarí, a location c. 20 km south of Talcahuca and where both species coexist. The experiment consisted of heating the area (a radius of 20 cm) around the home scar where adult individual limpets (shell length [SL]: 2.8–3.1 cm) of both species rest during daytime low tide. We heated the microsites with a propane torch for 5–8 min, with a maximum range of 45–50°C. Thirty individual limpets of each species were used for heating, and other 30 limpets were used as controls (no heating). We used infrared thermography as a noncontact and noninvasive method of temperature measurement (Chaperron & Seuront, 2011). We obtained thermal photographs of limpets and their microsites at the start and at the end of each assay using a Fluke Ti25 thermal imager (Fluke Corporation, Everett, WA, USA, sensitivity  $\leq 0.1$  at 30°C, accuracy is  $\pm 2^\circ\text{C}$ ). Air and seawater temperature were recorded in parallel. Behavioural responses (e.g. shell movement, displacements) and mortality were recorded during the assay.

## 2.5 | Biomass, shell carbonate content, and length

Animals were characterized in terms of maximal SL (mm) and comparisons among local populations were made using ANOVA. Shells and soft parts were separated and dried at 60°C overnight and then weighed (Shimadzu<sup>®</sup> analytical balance model AUX220; precision 0.001 g). Later, shells and tissues were calcinated at 600°C to remove organic content; the remnants were weighed and ash-free dry weight (AFDW) was calculated by subtracting from dry tissue weight. Shell weights after calcination were regarded as a proxy of the carbonate content of the shells (Ramajo et al., 2016). We also calculated the condition index (CI) for each individual as the ratio

between dry tissue to dry shell weight ( $\times 100$ ). We tested for differences in AFDW, carbonate content in shell (CaCO<sub>3</sub>) and CI between local populations using analysis of covariance (ANCOVA), with the maximum SL as covariate. We tested for differences in slopes (b), intercepts (a), and compared the response variable at the mean value of the covariate using least squares means (LSM) estimation. All analyses were done using log<sub>10</sub> transformed (SL, AFDW and CaCO<sub>3</sub>) and arcsine transformed (CI) data using MINITAB 14.

## 2.6 | Metabolic rate

A total of 120 adult limpets of each species were acclimated to experimental temperatures ( $T_{\text{hab}} = 14^\circ\text{C}$ ), and at the end of the 1 month acclimation period metabolic rate (MR) and heart rate (HR) were measured in all individuals. MR was estimated using a Microx optic fibre O<sub>2</sub>-meter (Presens Inc, DE) connected to a recirculating water bath by a flow-through cell housing (Presens Inc, DE). An acrylic respirometry chamber of 113 ml was used for respirometric analysis. The optic fibre was calibrated in a solution saturated with Na<sub>2</sub>O<sub>3</sub>S (0% air saturation) and in aerated ASW (100% air saturation). After calibration, oxygen availability (% air saturation) was measured in seawater for 60 min (recorded every 5 s). The first and the last 5 min were discarded to avoid possible disturbances from fibre manipulation, thus oxygen estimations are the average of the remaining 50 min of measurements. Body mass (Mb) was recorded before and after each measurement and the average of both Mb measurements was used in statistical analyses. Oxygen consumption (mg) was standardized by unit of time (h), volume (L), and wet weight (g) of the animal.

## 2.7 | Thermal performance curves

Thermal effects on physiological performance were estimated for populations of *S. viridula* and *S. zebrina* from all selected locations within their geographical range (three for *S. zebrina* and four for *S. viridula*). We used HR (cardiac activity) as a proxy of the relationship between organismal performance and  $T_{\text{hab}}$  (Chelazzi, Williams, & Gray, 1999). A total of 120 and 90 adult individuals (30 limpets for each population and species) were selected for analyses of thermal sensitivity using thermal performance curves (TPCs) for HR, which are described in terms of four parameters: (a) the optimal temperature ( $T_{\text{opt}}$ ); (b) the thermal breadth ( $T_{\text{br}}$ ); (c) the maximal performance ( $\mu_{\text{max}}$ ); and (d) the upper and lower limits of temperature at which the HR decreases ( $CT_{\text{min}}$  and  $CT_{\text{max}}$ ) (Angilletta, 2009). For each aerial temperature, treatment animals were exposed separately in plastic chambers with six subdivisions (200  $\times$  200  $\times$  100 mm), installed in a thermo-regulated bath at constant sea water temperature ( $\pm 0.5^\circ\text{C}$ , LWB- 122D, LAB TECH) for 30 min. We randomized the order of temperature trials for each individual and ensured at least 24 hr of rest between trials. Experimental temperatures for TPCs were chosen between  $-2$  and  $38^\circ\text{C}$ . For extreme temperatures of the thermal treatment ( $-2$  to  $6^\circ\text{C}$  and  $26$ – $38^\circ\text{C}$ ), HR was measured every  $1^\circ\text{C}$ , whereas for intermediate temperatures ( $6$ – $26^\circ\text{C}$ ) it was measured

every 2°C. HR was estimated using an AMP 03 heartbeat amplifier (Newshift Ltd®) connected to an oscilloscope and the results were expressed in beats per min<sup>-1</sup> (Gaitán-Espitia et al., 2014). Measurements of aerial cardiac activity were performed at the same period of the day to cancel the effects of a possible circadian or tidal rhythm of respiration. The mean HR for each limpet at each experimental temperature was calculated with the aim of estimating the TPCs for each population. We used the TABLECURVE2D curve-fitting software (5.01; Systat Software, Inc.) for model fitting. TPC parameters ( $\mu_{\max}$ ,  $T_{\text{opt}}$ ,  $CT_{\min}$  and  $CT_{\max}$ ) were extracted from the best models (see below for details). The ecophysiological characteristics of critical thermal maximum ( $CT_{\max}$ ) and minimum ( $CT_{\min}$ ) were derived numerically as the intersection points of the resulting TPC with the temperature axis ( $\mu = 0$ ). Temperature breadth ( $T_{\text{br}}$ ) for each population was calculated with the mean values of HR for each experimental temperature using the following equation (Gilchrist, 1995):

$$T_{\text{br}} = \sqrt{\sum_{i=1}^N \left[ \frac{\mu_i (T_i - T_{\text{opt}})}{\mu_{\max}} \right]^2}$$

where  $N$  is the number of temperatures,  $\mu_i$  is the mean HR at temperature  $T_i$ , and  $\mu_{\max}$  is the maximal performance.

### 3 | RESULTS

#### 3.1 | Variability of in situ seawater temperature, historical air temperature, and carbonate system parameters

The MODIS image of long-term SST variance (Figure 1a) shows that the nearshore area between Los Molles and Talcaruca is exposed to greater variance in SST than the region equatorward of the biogeographical break, and south of Los Molles, where a more stable temperature regime is observed (Figure 1a). Historical air temperature records from 14 coastal locations encompassing a large fraction of the geographical range of both species (Figure 1a inset, Supporting Information Table S1) showed a significant linear latitudinal gradient ( $R^2 = 0.973$ ,  $p < 0.001$ ) where temperatures ranged between 18.7°C at Arica (18.46° S) to 10.7°C at Punta Corona (41.78° S). In contrast to the smooth latitudinal pattern of coastal air temperatures and in agreement with the heterogeneity observed in satellite SST variance, we observed a discontinuity in the latitudinal gradient in annual mean and range of in situ SST across our study region (see Figure 1b). Temperature climatology across all study sites (Figure 1b), with ECIM as a surrogate for El Tabo, showed colder ocean temperature at Talcaruca year-round, with a two-degree difference compared to the next location equatorward (Huasco, black line). Similarly, the two poleward locations, Los Molles (red line) and ECIM (green line), were also year-round warmer than Talcaruca, particularly during spring and summer, with ECIM warmer than Los Molles from spring to autumn. The differences in temporal variability are also apparent in the climatology, with Talcaruca and Huasco showing stable patterns year-round and Los Molles and ECIM showing abrupt

seasonal transitions. Physical–chemical conditions across all study sites showed major variations (Table 1). Upwelling around PLV (30°14' S) was associated with notable differences between study sites in  $pH_T$ , SST, SSS,  $pCO_2$ , and saturation states ( $\Omega$ ) of aragonite and calcite, whereas  $A_T$  and DO did not show these contrasting differences between sites (Table 1). In addition, we observed at the Talcaruca site, in the vicinity of PLV, events of extremely high  $pCO_2$ , with coastal waters reaching values up to 1,600  $\mu\text{atm}$  and pH values as low as 7.6.

#### 3.2 | Behavioural responses

Body temperatures (BT) showed significant Treatment  $\times$  Species interaction ( $MS = 1574$ ,  $F_{1,89} = 22.5$ ,  $p < 0.001$ ). No significant difference between treatments was observed for *S. viridula* (Figure 2a, diff = 0.2916;  $p = 0.992$ ), while *S. zebrina* attained significantly higher BT in the heating treatment compared to the no-heating (control) treatment (Figure 2b post hoc Tukey HSD: diff = 19.67;  $p < .001$ ). BT responses to the heating treatment, an increase of about 45–50°C in the surrounding environment, differed significantly between the limpet species with *S. zebrina* reaching a significantly higher BT (Supporting Information Table S2, diff = 16.14;  $p < 0.001$ ).

#### 3.3 | Shell length, biomass, and carbonate content

Individuals from the different populations of each species showed significant differences in SL (*S. viridula*:  $F_{3,113} = 5.48$ ;  $p = 0.001$ ; *S. zebrina*:  $F_{2,98} = 13.81$ ;  $p < 0.001$ , Figure 3). For *S. viridula*, SL of limpets from the equatorward populations (Huasco, Talcaruca) was larger than for limpets collected in central Chile (Los Molles, El Tabo; Tukey pairwise comparison,  $p < 0.05$ , Figure 3a). For *S. zebrina*, SL from the Los Molles population was larger than for limpets from Talcaruca and the polewardmost (El Tabo) site (Figure 3b). Comparing these response variables at the mean value of the covariate SL (*S. viridula* = 32 mm  $\pm$  1.4 SE; 1.51  $\pm$  0.15 SE in log scale; *S. zebrina* = 27.4 mm  $\pm$  1.41; 1.44  $\pm$  0.13 in log scale), the results indicated significantly increased biomass (AFDW) of the *S. viridula* population from Talcaruca compared to Los Molles (Figure 3a, Table 2). However, the  $\text{CaCO}_3$  content of the *S. viridula* shells was lower in northern populations and showed a gradual but significant increase towards southern populations, with a maximum recorded in limpets collected from the recently colonized southernmost population (Figure 3a). The limpet *S. zebrina* is not present in our northernmost study site (Huasco), and the other local populations showed significant differences in AFDW, with lower values recorded in the northernmost population (Figure 3b). The  $\text{CaCO}_3$  content of shells showed a similar pattern, with increased values for the two southern populations (Figure 3b). Both species showed significant scaling relationships. AFDW,  $\text{CaCO}_3$  content and CI of *S. viridula* exhibited a significant scaling relationship with the maximum SL (Table 2). Apart from  $\text{CaCO}_3$  content in *S. zebrina* and CI for both species, which showed similar slopes but different intercepts, these relationships

**TABLE 1** Salinity, pH, and carbonate system parameters mean conditions ( $\pm$ SD) measured at the four study locations. The values correspond to nine discrete samples collected during the field period (February–December 2015). The symbol  $p$  indicates partial pressure of  $\text{CO}_2$  and  $\Omega$  indicates the saturation state for two biogenic forms of  $\text{CaCO}_3$

Carbonate system parameter	Huasco	Talcaruca	Los Molles	El Tabo
Salinity (PSU)	34.50 $\pm$ 0.10	34.38 $\pm$ 0.17	34.22 $\pm$ 0.20	33.45 $\pm$ 0.26
pH <sub>NBS</sub>	8.15 $\pm$ 0.12	7.90 $\pm$ 0.41	8.11 $\pm$ 0.14	8.01 $\pm$ 0.11
Total alkalinity (mM kg <sup>-1</sup> SW)	2,235.18 $\pm$ 20.02	2,279.60 $\pm$ 64.34	2,225.86 $\pm$ 30.21	2,264.10 $\pm$ 48.76
DIC (mM kg <sup>-1</sup> SW)	2,045.13 $\pm$ 82.65	2,158.18 $\pm$ 146.46	2,037.89 $\pm$ 145.13	2,127.68 $\pm$ 75.68
CO <sub>3</sub> (mM kg <sup>-1</sup> SW)	155.26 $\pm$ 60.22	103.21 $\pm$ 39.66	144.26 $\pm$ 34.81	108.99 $\pm$ 20.66
pCO <sub>2</sub> ( $\mu$ atm)	420.11 $\pm$ 122.12	879.91 $\pm$ 332.34	454.09 $\pm$ 176.07	642.87 $\pm$ 119.04
$\Omega_{\text{calcite}}$	3.96 $\pm$ 1.02	2.51 $\pm$ 0.95	3.51 $\pm$ 1.59	2.65 $\pm$ 0.50
$\Omega_{\text{aragonite}}$	2.55 $\pm$ 0.82	1.60 $\pm$ 0.59	2.24 $\pm$ 1.01	1.79 $\pm$ 0.32

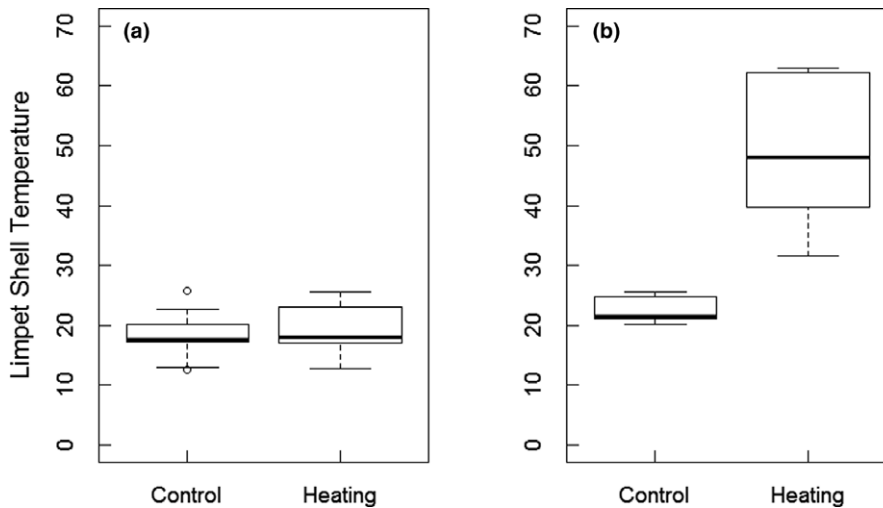


**FIGURE 2** Box plot of the body temperature of control and experimentally heated *Scurria viridula* (a) and *Scurria zebrina* (b) individuals. Black bars inside each box are the median, with the boxes containing the hinge (25%–75% quartile), and upper and lower lines indicating 1.5 times the hinge. Points outside the interval (outliers) are represented as dots. Heated individuals were exposed to 45–50°C for 3 min

exhibited significant differences in slope and intercept between studied populations (Table 2, Supporting information, Figures S1 and S2). Variation in biomass and shell  $\text{CaCO}_3$  content is integrated in the CI (i.e. biomass to shell weight ratio), which is a decreasing and significant function of the SL of *S. viridula* and *S. zebrina* (Figure 4a and b, respectively). Individuals of both species from populations collected at the southernmost location (El Tabo) showed significantly lower values of CI compared to the populations at the mean value of SL. No significant differences in CI were found between limpet populations from the other populations northward.

### 3.4 | Thermal performance curves

The best-fit models describing the TPCs of *S. viridula* and *S. zebrina* populations (Table 3) revealed the usual left-skewed shape of TPC (Figure 5 and Supporting Information Tables S3 and S4). We found significant differences among populations of *S. viridula* for the lower ( $\text{CT}_{\text{min}}$ , Table 3, one-way ANOVA,  $\text{CT}_{\text{min}}$ :  $F_{3,51} = 219.93$ ,  $p < 0.001$ ) and higher aerial temperature ( $\text{CT}_{\text{max}}$ , Table 3, one-way ANOVA,  $\text{CT}_{\text{max}}$ :  $F_{3,51} = 4.6726$ ;  $p = 0.0058$ ) where HR decreased. Differences followed a spatial trend, with higher  $\text{CT}_{\text{min}}$  and  $\text{CT}_{\text{max}}$

for *S. viridula* populations within the geographical range compared to range edge populations (see Table 3 and Figure 5a). A patchy pattern was observed among populations of *S. zebrina*, which did show significant differences between populations (Table 3, one-way ANOVA,  $\text{CT}_{\text{min}}$ :  $F_{2,92} = 0.602$ ,  $p = 0.44$ ;  $\text{CT}_{\text{max}}$ :  $F_{2,92} = 0.001$ ;  $p = 0.978$ , Figure 5b) with minimal values of  $\text{CT}_{\text{max}}$  and  $\text{CT}_{\text{min}}$  in individuals from the El Tabo population. The thermal optimum ( $T_{\text{opt}}$ ) showed a similar pattern with significant differences among populations of *S. viridula*, which showed decreasing  $T_{\text{opt}}$  towards the range edge (Table 3, one-way ANOVA,  $F_{3,51} = 3.32$ ,  $p = 0.00267$ ). *Scurria zebrina* did not show lower  $T_{\text{opt}}$  at the range edge, or a gradient-like response (Table 3, one-way ANOVA,  $F_{2,92} = 0.034$ ,  $p = 0.8537$ ). We found no significant differences in thermal breadth ( $T_{\text{br}}$ ) among populations in either *Scurria* species (Table 3, one-way ANOVA,  $F_{3,51} = 0.96$ ,  $p = 0.822$  and  $F_{1,35} = 0.93$ ,  $p = 0.644$  for *S. viridula* and *S. zebrina*, respectively). Interestingly, thermal breadth was 2–4°C higher for *S. zebrina* compared to *S. viridula* in all studied populations (Table 3). Maximal performance ( $\mu_{\text{max}}$ ) in *S. viridula* decreased monotonically towards its leading range edge and showed significant differences among populations (one-way ANOVA;  $F_{3,51} = 3.82$ ;  $p = 0.0151$ ), while  $\mu_{\text{max}}$  in *S. zebrina* increased

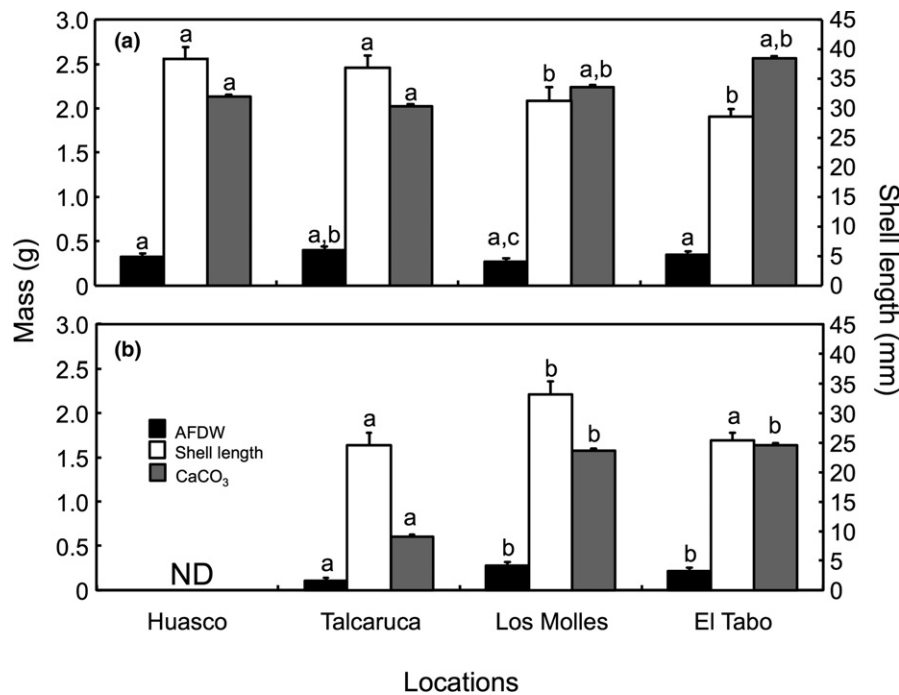


**FIGURE 3** Least squares mean (LSM  $\pm$  SE) of ash-free dry weight (AFDW), carbonate content ( $\text{CaCO}_3$ ), and shell length (mean  $\pm$  SD) recorded in shells of (a) *Scurria viridula* and (b) *Scurria zebrina* collected in our study populations. LSM is the predicted value of AFDW and  $\text{CaCO}_3$  at the mean value of the covariate, shell length, and was estimated using ANCOVA analysis. Shell length was compared across sites using ANOVA. Different letters above the bars (a–c) indicate significant differences between pairs of populations using Tukey post hoc pairwise comparisons for each variable (AFDW, shell length, and carbonate content)

**TABLE 2** Summary of ANCOVA testing for equal (Population  $\times$  Shell Length) and separate (Shell Length [Population]) slopes for the regression between Ash-Free Dry Weight (AFDW), Carbonate content ( $\text{CaCO}_3$ ) and Condition Index with maximum shell length. Significant differences are depicted in bold

Species	Variable	Source of variation							
		Population $\times$ Shell Length				Shell Length(Population)			
		DF <sub>(source, error)</sub>	MS	F	P	DF <sub>(source, error)</sub>	MS	F	p
<i>S. viridula</i>	AFDW (g)	3, 102	0.120	3.86	<b>0.012</b>	4, 102	64.10	205.54	<b>&lt;0.001</b>
	$\text{CaCO}_3$ (g)	3, 105	0.037	3.52	<b>0.018</b>	4, 105	44.34	419.29	<b>&lt;0.001</b>
	Condition Index (%)	3, 109	0.011	0.004	0.550	4, 109	0.49	75.23	<b>&lt;0.001</b>
<i>S. zebrina</i>	AFDW (g)	2, 93	0.338	6.75	<b>0.002</b>	3, 93	3.41	68.13	<b>&lt;0.001</b>
	$\text{CaCO}_3$ (g)	2, 92	0.099	0.96	0.386	3, 92	3.66	35.64	<b>&lt;0.001</b>
	Condition Index (%)	2, 93	0.004	0.19	0.827	3, 93	0.69	36.63	<b>&lt;0.001</b>

significantly in Los Molles compared to the Talcaruca and El Tabo populations (Table 3, one-way ANOVA,  $F_{2,92} = 9.392$ ;  $p = 0.0041$ ). Hence, the height of the TPCs (CI 95 for latitude:  $\mu_{\max} = -0.11$ , 2.46) but not their amplitude (CI 95 for latitude:  $T_{br} = 2.12$ , 8.21) changed across latitude in both species (Figure 5a,b).

### 3.5 | Metabolic rate

Metabolic rate, measured as volume of oxygen consumed by individuals (hereafter  $\text{VO}_2$ ), varied significantly among localities (one-way ANCOVA  $F_{3,107} = 5.737$ ;  $p = 0.0011$ ) for *S. viridula*.

Minimum values of  $\text{VO}_2$ ,  $0.15 \pm 0.064 \text{ mg O}_2 \text{ L}^{-1}$ , were found in individuals from the polewardmost population, El Tabo (Figure 6). The equatorward populations of *S. viridula* (i.e. Huasco and Talcaruca) exhibited higher values in  $\text{VO}_2$  but differences between localities were not significant (a posteriori Tukey HSD,  $p = 0.179$ , for paired comparisons). Values of  $\text{VO}_2$  for individuals of *S. zebrina* from Los Molles and Talcaruca showed significant differences with those from the El Tabo population (one-way ANCOVA  $F_{2,115} = 12.331$ ;  $p < 0.001$ ), thus individuals from El Tabo showed significantly lower MR than the other populations of *S. zebrina* (Figure 6).

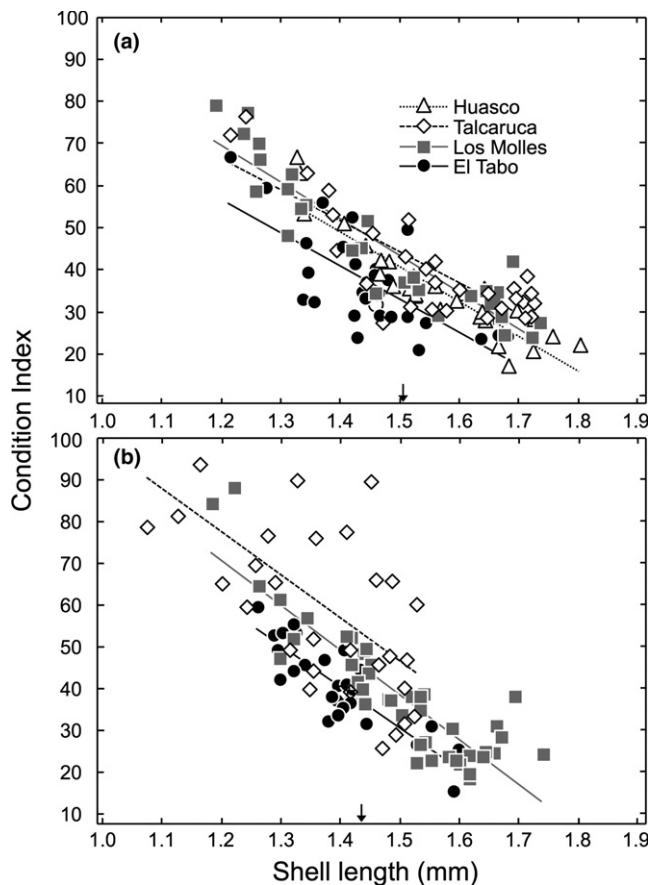


**FIGURE 4** Bivariate relationship of condition index (dry biomass/shell mass  $\times$  100) and shell length of (a) *Scurria viridula* and (b) *Scurria zebrina*. The arrow above the x-axis indicates the mean value of the covariate, shell length. Comparison of slopes and intercepts between these relationships was based on ANCOVA (see Table 3) and a least squares mean comparison, i.e. comparing the fitted value for each regression line at the mean value of the covariate, shell length. Proportional data of the condition index were arcsine transformed to meet ANCOVA assumptions

## 4 | DISCUSSION

Our study documented contrasting plastic phenotypic responses between populations of the leading edge species, *S. viridula*, and *S. zebrina*, the rear edge species, across the biogeographical boundary where their geographical distributions overlap. Contrasts were reflected across the range of phenotypic traits examined and in the different spatial structure of between-population responses for the two species. The phenotypic response of range edge populations of both species, at El Tabo for *S. viridula* and at Talcaruca for *S. zebrina*, was significantly different from populations inside the range of either species. In agreement with theoretical expectations the plastic, between-site, phenotypic responses for the species at the leading edge of its range were gradient-like or did not show significant differences, while the response of rear edge populations was site-specific (Lourenco et al., 2016; Nicastro et al., 2013; Zardi et al., 2015). Together with the heterogeneous and extreme physical and chemical

conditions, we documented in the intertidal and coastal zone around PLV (i.e.  $\sim 30^\circ$  S, Torres et al., 2011), it becomes apparent that local environmental conditions can play an important role in the maintenance of coastal marine biogeographical breaks in upwelling regions.

### 4.1 | Physiological responses at the leading versus rear edge of the *Scurria* limpets

Both species showed a reduced performance in AFDW,  $\text{CaCO}_3$  content, CI, and MR towards the edges of their respective ranges and clear negative responses at Talcaruca, located in close proximity to the PLV biogeographical break (Figure 1a). The spatial pattern of different physiological responses highlights the role of ocean chemistry (e.g.  $p\text{CO}_2$  and  $\Omega$ ) and the interactive effects that multiple stressors can have on the performance of invertebrate species (Duarte et al., 2014; Williams et al., 2011). Individuals from Talcaruca were generally smaller in size and had lower biomass than individuals from the other populations, a contrast that was most significant with the site immediately south (Los Molles, see Figures 3 and 6). These between-site contrasts indicate that individuals at Talcaruca compromised their growth in coping with stressful conditions. It is likely that SST is an important driver determining limpet distribution across large scales (e.g. *Patella vulgata*, Seabra et al., 2016). More than 50% of the limpet body is in close contact with rock; substrate heating can also play a role in local individual performance, and body and substrate temperatures are expected to be directly correlated (Chappon & Seuront, 2011).

Many gastropods are able to cope with thermally stressful local conditions through behavioural thermoregulation, taking refuge in cooler microhabitats (e.g. *Cellana grata* (Williams & Morrill, 1995); *Nerita atramentosa* (Chappon & Seuront, 2011)). Under experimental substrate heating, *S. viridula* actively escaped while *S. zebrina* clamped to the rock, similar to their behavioural responses under predation threat (Espoz & Castilla, 2000). This observation was in agreement with differences in shell temperature after substrate heating experiments (Figure 2) and heat avoidance behaviour can reconcile the observation of higher across-site  $\text{CT}_{\text{max}}$  values for *S. zebrina*. Similarly, at the sites where *S. zebrina* coexists with *S. viridula*, its  $T_{\text{opt}}$  values are always higher, but they lie very close to its  $\text{CT}_{\text{max}}$  values.

These results are an extension of earlier findings showing that altitudinal persistence of tropical or montane species is compromised by narrow thermal safety margins (Huey et al., 2009; Sunday et al., 2014). Namely, populations of *S. viridula* that maintain their aerobic capacity at warmer temperatures are expected to have higher thermal tolerance and are predicted to persist longer than populations that experienced a decline in aerobic performance as temperature increases, like *S. zebrina* (Gaitán-Espitía et al., 2014). Our results allow us to extend the thermal safety margin hypothesis to populations at the rear edge of the range, which reach higher temperatures only by compromising their thermal safety margin, something that is also suggested by the  $\mu_{\text{max}}$ . Finally, coexistence between highly related species, such as our two focal species, may be influenced by spatial niche differentiation driven by habitat suitability or even

**TABLE 3** Parameters of thermal performance curves ( $\pm$ SD) in populations of the limpets *Scurria viridula* and *Scurria zebrina*. Abbreviations are as follows: minimum and maximum critical temperature ( $CT_{min}$  and  $CT_{max}$ , respectively), optimal temperature ( $T_{opt}$ ), maximal performance ( $\mu_{max}$ ), and thermal breadth ( $T_{br}$ )

Population	$CT_{min}$ (°C)	$CT_{max}$ (°C)	$T_{opt}$ (°C)	$\mu_{max}$	$T_{br}$
<i>S. viridula</i>					
Huasco	4.22 $\pm$ 0.44	37.07 $\pm$ 6.34	28.74 $\pm$ 1.09	80.78 $\pm$ 5.36	27.18 $\pm$ 7.75
Talcaruca	2.08 $\pm$ 10.68	36.49 $\pm$ 8.41	27.85 $\pm$ 1.22	68.42 $\pm$ 5.99	28.16 $\pm$ 3.49
Los Molles	-0.21 $\pm$ 0.41	34.57 $\pm$ 5.22	26.18 $\pm$ 0.97	66.12 $\pm$ 4.76	27.59 $\pm$ 6.38
El Tabo	-0.99 $\pm$ 0	34.11 $\pm$ 2.92	23.45 $\pm$ 1.41	51.55 $\pm$ 6.92	27.03 $\pm$ 8.12
<i>S. zebrina</i>					
Talcaruca	0.005 $\pm$ 0.12	36.44 $\pm$ 0.27	31.46 $\pm$ 2.72	52.51 $\pm$ 3.75	29.18 $\pm$ 7.19
Los Molles	0.001 $\pm$ 0.10	36.50 $\pm$ 0.35	32.28 $\pm$ 3.48	71.21 $\pm$ 4.81	30.44 $\pm$ 9.30
El Tabo	-0.199 $\pm$ 0.01	32.11 $\pm$ 1.74	27.64 $\pm$ 2.02	52.05 $\pm$ 1.59	29.88 $\pm$ 9.14

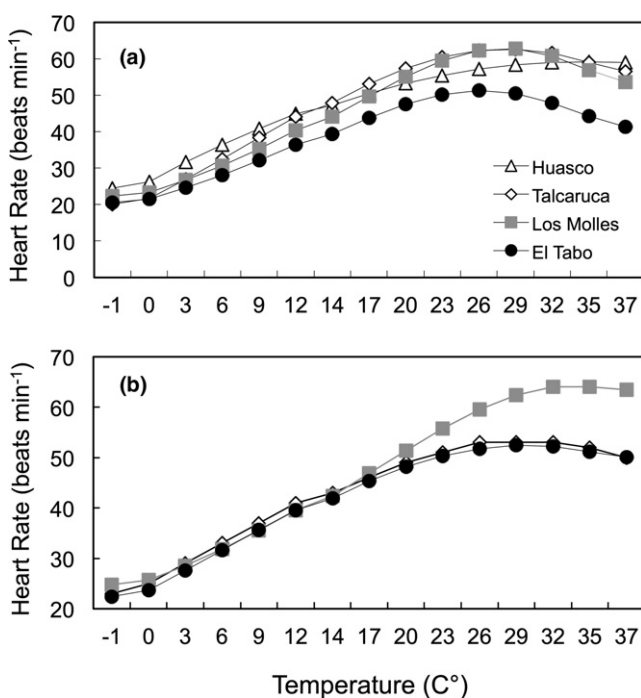


**FIGURE 5** Comparison of thermal performance curves (TPC) during aerial exposure for (a) *Scurria viridula* and (b) *Scurria zebrina* fitted using density distributions selected using AIC (see Supporting Information Tables S3 and S4 for details)

competition. Notably, and in contrast to this expectation, our results suggest that a temperature-driven behavioural mechanism alone may produce the small-scale segregation pattern observed at the experimental site in the range overlap region (Aguilera et al., 2013).

#### 4.2 | Coastal upwelling circulation as a biogeographical barrier

The smooth latitudinal gradient in coastal air temperatures observed along the coast of Chile (Lardies et al., 2011) contrasts with the local heterogeneity in ocean temperature driven by coastal upwelling (Navarrete, Wieters, Broitman, & Castilla, 2005). The PLV headland

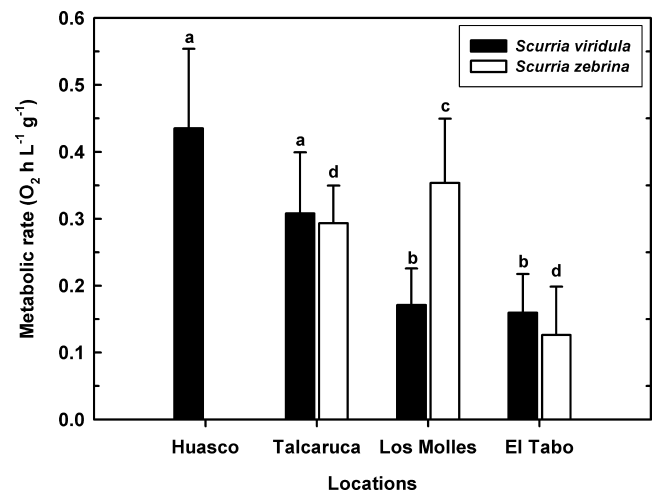


**FIGURE 6** Mass-specific rate of oxygen uptake ( $VO_2$  in  $h L^{-1} g^{-1}$ ) in seawater by the limpets *Scurria zebrina* and *Scurria viridula* at four study sites along the north-central Chilean coast. Mean  $\pm$  SE is indicated. Significant differences between population are indicated by different letters (a–d) over each bar for Tukey post hoc pairwise comparisons within species

marks the transition between an area characterized by weak and persistent upwelling to a region poleward, between 29° and 39° S, dominated by strong and variable upwelling-favourable conditions (Hormazabal, Shaffer, & Leth, 2004). The environmental setting we detected around the PLV oceanographic transition mirrors the drivers of biogeographical structure highlighted for similar transitions along western North America (Fenberg, Menge, Raimondi, & Rivadeneira, 2014), which bears important implications. Observations along the California and Humboldt coasts (Iles et al., 2012; Sydeman et al., 2014), together with current projections for mid-latitude upwelling regions worldwide (Ryckaczewski et al., 2015), indicate that wind maxima will be displaced poleward, while alongshore winds will intensify in a warmer climate (Bakun, 1990). Hence, future climate seems poised to alter coastal upwelling circulation patterns; for instance some scenarios involve larger and more homogeneous areas under the influence of upwelling waters, together with stronger and longer periods of offshore surface water transport (Iles et al., 2012;

Wang, Gouhier, Menge, & Ganguly, 2015) and cooler air temperatures onshore (Falvey & Garreaud, 2009).

On the other hand, an intensified upwelling regime will expose coastal species to demanding physical and chemical ocean conditions, particularly for planktonic larvae (Doney et al., 2012; Waldbusser et al., 2013). It is interesting to note that patellogastropod limpets have short larval durations and the phylogeographical (Ewers-Saucedo et al., 2016; Haye et al., 2014) or biogeographical breaks documented around PLV are chiefly of algae or species with short pelagic larval periods, similar to the rocky shores of the north-eastern Pacific (Fenberg et al., 2014; Pelc, Warner, & Gaines, 2009).

Together, our observational and experimental results suggest that environmental conditions around large upwelling centres constrain local population performance of adult individuals. Coastal upwelling can impose metabolic costs on larval stages of calcifying organisms (Waldbusser et al., 2013), which complements flow-driven mechanistic drivers of biogeographical breaks (Gaylord & Gaines, 2000; Pappalardo, Pringle, Wares, & Byers, 2014). Persistent and strong upwelling around PLV (Navarrete et al., 2005; Torres et al., 2011) can also underpin the rapid parapatric divergence in adaptive physiological/behavioural responses between our focal species, which are end members of their clade (Espoz et al., 2004). Key physiological and life history characteristics of molluscs will be impacted by the increased levels of ocean acidification and warming brought about by global climate change in the ocean (Gattuso et al., 2015). Hence, our results are in accordance with the observation that future ocean acidification may delay development rates at critical early life stages of calcifying organisms. These changes could restrict larval dispersal for multiple species (Kroeker, Kordas, Crim, & Singh, 2010), while opening opportunities for others (Lourenco et al., 2016). Using a combination of ecological, physiological, and molecular approaches may prove to be the best means of detecting multiple impacts of climate change (Moritz & Agudo, 2013). This integrated approach may play an important role in understanding the heterogeneous responses of populations living at the leading and rear edges of their ranges, helping us improve and guide conservation and management efforts.

## ACKNOWLEDGEMENTS

Financial support was provided by FONDECYT grants to MAL (1140092), NAL (1140938), BRB (1181300) and MAA (1160223), who also acknowledges support from PAI-CONICYT 79150002. Additional support was provided by the ICM centre for the study of MULTiple drivers of marine Socio-Ecological Systems (MUSELS) and PIA CONICYT ACT172037. All experiments were conducted according to current Chilean law. The authors declare to have no conflict of interest.

## DATA ACCESSIBILITY

All MODIS Satellite data used in this study are available through the ocean colour website (<https://oceandata.sci.gsfc.nasa.gov/>) and

in situ temperature records are available from the ceazamet platform ([www.ceazamet.cl](http://www.ceazamet.cl))

## ORCID

Bernardo R. Broitman  <http://orcid.org/0000-0001-6582-3188>

## REFERENCES

- Aguilera, M. A., Valdivia, N., & Broitman, B. R. (2013). Spatial niche differentiation and coexistence at the edge: Co-occurrence distribution patterns in *Scurria* limpets. *Marine Ecology Progress Series*, 483, 185–198. <https://doi.org/10.3354/meps10293>
- Angilletta, M. J. Jr. (2009). *Thermal adaptation: a theoretical and empirical synthesis*. New York, NY: Oxford University Press.
- Aravena, G., Broitman, B. R., & Stenseth, N. C. (2014). Twelve years of change in coastal upwelling along the central-northern coast of Chile: Spatially heterogeneous responses to climatic variability. *PLoS ONE*, 9, e90276. <https://doi.org/10.1371/journal.pone.0090276>
- Bakun, A. (1990). Global climate change and intensification of coastal ocean upwelling. *Science*, 247, 198–201. <https://doi.org/10.1126/science.247.4939.198>
- Blanchette, C. A., Miner, C. M., Raimondi, P. T., Lohse, D., Heady, K. E. K., & Broitman, B. R. (2008). Biogeographical patterns of rocky intertidal communities along the Pacific coast of North America. *Journal of Biogeography*, 35, 1593–1607. <https://doi.org/10.1111/j.1365-2699.2008.01913.x>
- Bowen, B. W., Gaither, M. R., DiBattista, J. D., Iacchei, M., Andrews, K. R., Grant, W. S., ... Briggs, J. C. (2016). Comparative phylogeography of the ocean planet. *Proceedings of the National Academy of Sciences of the United States of America*, 113, 7962–7969. <https://doi.org/10.1073/pnas.1602404113>
- Brown, J. H., Stevens, G. C., & Kaufman, D. M. (1996). The geographic range: Size, shape, boundaries, and internal structure. *Annual Review of Ecology and Systematics*, 27, 597–623. <https://doi.org/10.1146/annurev.ecolsys.27.1.597>
- Chappon, C., & Seuront, L. (2011). Behavioral thermoregulation in a tropical gastropod: Links to climate change scenarios. *Global Change Biology*, 17, 1740–1749. <https://doi.org/10.1111/j.1365-2486.2010.02356.x>
- Chelazzi, G., Williams, G. A., & Gray, D. R. (1999). Field and laboratory measurement of heart rate in a tropical limpet, *Cellana grata*. *Journal of the Marine Biological Association of the UK*, 79, 749–751. <https://doi.org/10.1017/S0025315498000915>
- Di Castri, F., & Hajek, E. (1976). *Bioclimatología de Chile*. Santiago, Chile: Vicerectoria Académica de la Universidad Católica de Chile.
- Doney, S. C., Ruckelshaus, M., Duffy, J. E., Barry, J. P., Chan, F., English, C. A., ... Talley, L. D. (2012). Climate change impacts on marine ecosystems. *Annual Review of Marine Science*, 4, 11–37. <https://doi.org/10.1146/annurev-marine-041911-111611>
- Duarte, C., Navarro, J. M., Acuña, K., Torres, R., Manríquez, P. H., Lardies, M. A., ... Aguilera, V. (2014). Combined effects of temperature and ocean acidification on the juvenile individuals of the mussel *Mytilus chilensis*. *Journal of Sea Research*, 85, 308–314. <https://doi.org/10.1016/j.seares.2013.06.002>
- Espoz, C., & Castilla, J. C. (2000). Escape responses of four Chilean intertidal limpets to seastars. *Marine Biology*, 137, 887–892. <https://doi.org/10.1007/s002270000426>
- Espoz, C., Lindberg, D. R., Castilla, J. C., & Simison, W. B. (2004). Los patellogastropodos intermareales de Chile y Perú. *Revista Chilena de Historia Natural*, 77, 257–283.
- Ewers-Saucedo, C., Pringle, J. M., Sepulveda, H. H., Byers, J. E., Navarrete, S. A., & Wares, J. P. (2016). The oceanic concordance of



- phylogeography and biogeography: A case study in *Notochthamalus*. *Ecology and Evolution*, 6, 4403–4420. <https://doi.org/10.1002/ece3.2205>
- Falvey, M., & Garreaud, R. D. (2009). Regional cooling in a warmer world: Recent temperature trends in the southeast Pacific and along the west coast of subtropical South America (1979–2000). *Journal of Geophysical Research – Atmospheres*, 114, D04102.
- Feely, R. A., Sabine, C. L., Hernandez-Ayon, J. M., Ianson, D., & Hales, B. (2008). Evidence for upwelling of corrosive “acidified” water onto the continental shelf. *Science*, 320, 1490–1492. <https://doi.org/10.1126/science.1155676>
- Fenberg, P. B., Menge, B. A., Raimondi, P. T., & Rivadeneira, M. M. (2014). Biogeographic structure of the northeastern Pacific rocky intertidal: The role of upwelling and dispersal to drive patterns. *Ecography*, 38, 83–95.
- Gaitán-Espitia, J. D., Bacigalupe, L. D., Opitz, T., Lagos, N. A., Timmermann, T., & Lardies, M. A. (2014). Geographic variation in thermal physiological performance of the intertidal crab *Petrolisthes violaceus* along a latitudinal gradient. *The Journal of Experimental Biology*, 4, 4379–4386. <https://doi.org/10.1242/jeb.108217>
- Gattuso, J.-P., Magnan, A., Bille, R., Cheung, W. W. L., Howes, E. L., & Joos, F. ... Turley, C. (2015). Contrasting futures for ocean and society from different anthropogenic CO<sub>2</sub> emissions scenarios. *Science*, 349, aac4722-1–aac4722-10.
- Gaylord, B., & Gaines, S. D. (2000). Temperature or transport? Range limits in marine species mediated solely by flow. *The American Naturalist*, 155, 769–789. <https://doi.org/10.1086/303357>
- Gilchrist, G. W. (1995). A quantitative genetic analysis of thermal sensitivity in the locomotor performance curve of *Aphidius ervi*. *Evolution*, 50, 1560–1572.
- Hampe, A., & Petit, R. J. (2005). Conserving biodiversity under climate change: The rear edge matters. *Ecology Letters*, 8, 461–467. <https://doi.org/10.1111/j.1461-0248.2005.00739.x>
- Haraldsson, C., Anderson, L. G., Hassellöv, M., Hulth, S., & Olsson, K. (1997). Rapid, high-precision potentiometric titration of alkalinity in ocean and sediment pore waters. *Deep-Sea Research Part I: Oceanographic Research Papers*, 44, 2031–2044. [https://doi.org/10.1016/S0967-0637\(97\)00088-5](https://doi.org/10.1016/S0967-0637(97)00088-5)
- Haye, P. A., Segovia, N. I., Muñoz-Herrera, N. C., Gálvez, F. E., Martínez, A., Meynard, A., ... Faugeron, S. (2014). Phylogeographic structure in benthic marine invertebrates of the Southeast Pacific coast of Chile with differing dispersal potential. *PLoS ONE*, 9, 1–15.
- Helmuth, B., Mieszkowska, N., Moore, P., & Hawkins, S. J. (2006). Living on the edge of two changing worlds: Forecasting the responses of rocky intertidal ecosystems to climate change. *Annual Review of Ecology, Evolution, and Systematics*, 37, 373–404. <https://doi.org/10.1146/annurev.ecolsys.37.091305.110149>
- Hewitt, G. (2000). The genetic legacy of the Quaternary ice ages. *Nature*, 405, 907–913. <https://doi.org/10.1038/35016000>
- Hill, H. E., Hickey, B. M., Shillington, F. A., Strub, P. T., Brink, K. H., Barton, E. D., & Thomas, A. C. (1998). Eastern ocean boundaries. Coastal segment. *The Sea*, 11, 29–67.
- Hormazabal, S., Shaffer, G., & Leth, O. (2004). Coastal transition zone off Chile. *Journal of Geophysical Research – Oceans*, 109, C01021.
- Huey, R. B., Deutsch, C. A., Tewksbury, J. J., Vitt, L. J., Hertz, P. E., Alvarez Pérez, H. J., & Garland, T. (2009). Why tropical forest lizards are vulnerable to climate warming. *Proceedings of the Royal Society B*, 276, 1939–1948. <https://doi.org/10.1098/rspb.2008.1957>
- Iles, A. C., Gouhier, T. C., Menge, B. A., Stewart, J. S., Haupt, A. J., & Lynch, M. C. (2012). Climate-driven trends and ecological implications of event-scale upwelling in the California Current System. *Global Change Biology*, 18, 783–796. <https://doi.org/10.1111/j.1365-2486.2011.02567.x>
- Kapsenberg, L., & Hofmann, G. E. (2016). Ocean pH time-series and drivers of variability along the northern Channel Islands, California, USA. *Limnology and Oceanography*, 61, 953–968. <https://doi.org/10.1002/lno.10264>
- Kawecki, T. J., & Ebert, D. (2004). Conceptual issues in local adaptation. *Ecology Letters*, 7, 1225–1241. <https://doi.org/10.1111/j.1461-0248.2004.00684.x>
- Kroeker, K. J., Kordas, R. L., Crim, R. N., & Singh, G. G. (2010). Meta-analysis reveals negative yet variable effects of ocean acidification on marine organisms. *Ecology Letters*, 13, 1419–1434. <https://doi.org/10.1111/j.1461-0248.2010.01518.x>
- Lardies, M. A., Muñoz, J. L., Paschke, K. A., & Bozinovic, F. (2011). Latitudinal variation in the aerial/aquatic ratio of oxygen consumption of a supratidal high rocky-shore crab. *Marine Ecology*, 32, 42–51. <https://doi.org/10.1111/j.1439-0485.2010.00408.x>
- Lima, F. P., Queiroz, N., Ribeiro, P. A., Hawkins, S. J., & Santos, A. M. (2006). Recent changes in the distribution of a marine gastropod, *Patella rustica* (Linnaeus, 1758), and their relationship to unusual climatic events. *Journal of Biogeography*, 33, 812–822. <https://doi.org/10.1111/j.1365-2699.2006.01457.x>
- Lourenco, C. R., Zardi, G. I., McQuaid, C. D., Serrao, E. A., Pearson, G. A., Jacinto, R., & Nicastro, K. R. (2016). Upwelling areas as climate change refugia for the distribution and genetic diversity of a marine macroalga. *Journal of Biogeography*, 43, 1595–1607. <https://doi.org/10.1111/jbi.12744>
- Moritz, R., & Agudo, C. (2013). The future of species under climate change: Resilience or decline? *Science*, 341, 504–508. <https://doi.org/10.1126/science.1237190>
- Navarrete, S. A., Wieters, E. A., Broitman, B. R., & Castilla, J. C. (2005). Scales of benthic-pelagic coupling and the intensity of species interactions: From recruitment limitation to top-down control. *Proceedings of the National Academy of Sciences of the United States of America*, 102, 18046–18051. <https://doi.org/10.1073/pnas.0509119102>
- Nicastro, K. R., Zardi, G. I., Teixeira, S., Neiva, J., Serrao, E. A., & Pearson, G. A. (2013). Shift happens: Trailing edge contraction associated with recent warming trends threatens a distinct genetic lineage in the marine macroalga *Fucus vesiculosus*. *BMC Biology*, 11, 6. <https://doi.org/10.1186/1741-7007-11-6>
- Pappalardo, P., Pringle, J. M., Wares, J. P., & Byers, J. E. (2014). The location, strength, and mechanisms behind marine biogeographic boundaries of the east coast of North America. *Ecography*, 38(7), 722–731.
- Pelc, R. A., Warner, R. R., & Gaines, S. D. (2009). Geographical patterns in the genetic structure in marine species with contrasting life histories. *Journal of Biogeography*, 36, 1881–1890. <https://doi.org/10.1111/j.1365-2699.2009.02138.x>
- Peterson, A. T., Soberón, J., Pearson, R. G., Anderson, R. P., Martínez-Meyer, E., Nakamura, M., & Araujo, M. B. (2011). *Ecological niches and geographic distributions*. Princeton, NJ: Princeton University Press.
- Pierrot, D., Lewis, E., & Wallace, W. R. (2006) MS Excel Program Developed for CO<sub>2</sub> System Calculations. ORNL/CDIAC-105a.
- Ramajo, L., Marbà, N., Prado, L., Peron, S., Lardies, M. A., Rodríguez-Navarro, A. B., ... Duarte, C. M. (2016). Biomineralization changes with food supply confer juvenile scallops (*Argopecten purpuratus*) resistance to ocean acidification. *Global Change Biology*, 22, 2025–2037. <https://doi.org/10.1111/gcb.13179>
- Rivadeneira, M. M., & Fernández, M. (2005). Shifts in southern endpoints of distribution in rocky intertidal species along the south-eastern Pacific coast. *Journal of Biogeography*, 32, 203–209. <https://doi.org/10.1111/j.1365-2699.2004.01133.x>
- Rykaczewski, R. R., Dunne, J. P., Sydemann, W. J., García-Reyes, M., Black, B. A., & Bograd, S. J. (2015). Poleward displacement of coastal upwelling-favorable winds in the ocean's eastern boundary currents through the 21st century. *Geophysical Research Letters*, 42, 6424–6431. <https://doi.org/10.1002/2015GL064694>
- Seabra, R., Wetthey, D. S., Santos, A. M., Gomes, F., & Lima, F. P. (2016). Equatorial range limits of an intertidal ectotherm are more linked to

- water than air temperature. *Global Change Biology*, 22, 3320–3331. <https://doi.org/10.1111/gcb.13321>
- Somero, G. N. (2010). The physiology of climate change: How potentials for acclimatization and genetic adaptation will determine “winners” and “losers”. *Journal of Experimental Biology*, 213, 912–920. <https://doi.org/10.1242/jeb.037473>
- Sunday, J. M., Bates, A. E., Kearney, M. R., Colwell, R. K., Dulvy, N. K., Longino, J. T., & Huey, R. B. (2014). Thermal-safety margins and the necessity of thermoregulatory behavior across latitude and elevation. *Proceedings of the National Academy of Sciences of the United States of America*, 111, 5610–5615. <https://doi.org/10.1073/pnas.1316145111>
- Sydesman, W. J., García-Reyes, M., Schoeman, D. S., Rykaczewski, R. R., Thompson, S. A., Black, B. A., & Bograd, S. J. (2014). Climate change and wind intensification in coastal upwelling ecosystems. *Science*, 345, 77–80. <https://doi.org/10.1126/science.1251635>
- Tapia, F. J., Largier, J. L., Castillo, M., Wieters, E. A., & Navarrete, S. A. (2014). Latitudinal discontinuity in thermal conditions along the near-shore of central-northern Chile. *PLoS ONE*, 9, 1–11.
- Torres, R., Pantoja, S., Harada, N., González, H. A., Daneri, G., Frangopolos, M., ... Fukawa, M. (2011). Air-sea CO<sub>2</sub> fluxes along the coast of Chile: From CO<sub>2</sub> outgassing in central northern upwelling waters to CO<sub>2</sub> uptake in southern Patagonian fjords. *Journal of Geophysical Research—Oceans*, 116, C0900.
- Waldbusser, G. G., Brunner, E. L., Haley, B. A., Hales, B., Langdon, C. J., & Prah, F. G. (2013). A developmental and energetic basis linking larval oyster shell formation to acidification sensitivity. *Geophysical Research Letters*, 40, 2171–2176. <https://doi.org/10.1002/grl.50449>
- Wang, D., Gouhier, T. C., Menge, B. A., & Ganguly, A. R. (2015). Intensification and spatial homogenization of coastal upwelling under climate change. *Nature*, 518, 390–394. <https://doi.org/10.1038/nature14235>
- Wetthey, D. S. (1983). Geographic limits and local zonation: The barnacles *Semibalanus (Balanus)* and *Chthamalus* in New England. *Biological Bulletin*, 165, 330–341. <https://doi.org/10.2307/1541373>
- Williams, G. A., De Pirro, M., Cartwright, S., Khangura, K., Ng, W. C., Leung, P. T. Y., & Morritt, D. (2011). Come rain or shine: The combined effects of physical stresses on physiological and protein-level responses of an intertidal limpet in the monsoonal tropics. *Functional Ecology*, 25, 101–110. <https://doi.org/10.1111/j.1365-2435.2010.01760.x>
- Williams, G. A., & Morritt, D. (1995). Habitat partitioning and thermal tolerance in a tropical limpet, *Cellana grata*. *Marine Ecology Progress Series*, 124, 89–103. <https://doi.org/10.3354/meps124089>
- Woods, H. A., Dillon, M. E., & Pincebourde, S. (2015). The roles of microclimatic diversity and of behaviour in mediating the responses of ectotherms to climate change. *Journal of Thermal Biology*, 54, 86–97. <https://doi.org/10.1016/j.jtherbio.2014.10.002>
- Zardi, G. I., Nicastrò, K. R., Serrao, E. A., Jacinto, R., Monteiro, C. A., & Pearson, G. A. (2015). Closer to the rear edge: Ecology and genetic diversity down the core-edge gradient of a marine macroalga. *Ecosphere*, 6, 1–25.

## BIOSKETCH

**Bernardo R. Broitman** is a Senior Researcher at the Centro de Estudios Avanzados en Zonas Áridas in Coquimbo, Chile. His expertise is on the processes defining the local and regional patterns of community organization on temperate rocky shores and is currently focused on the effects of climatic variability on regional ecological dynamics and the biogeography of coastal upwelling regions.

## SUPPORTING INFORMATION

Additional supporting information may be found online in the Supporting Information section at the end of the article.

**How to cite this article:** Broitman BR, Aguilera MA, Lagos NA, Lardies MA. Phenotypic plasticity at the edge: Contrasting population-level responses at the overlap of the leading and rear edges of the geographical distribution of two *Scurria* limpets. *J Biogeogr.* 2018;00:1–12. <https://doi.org/10.1111/jbi.13406>